Electronic Supplementary Material (ESI) for ChemComm.

Supporting Information

Photo-activation of d^0 Niobium imido azides: en route to nitrido complexes

Clément Camp, Lauren Grant, Robert G. Bergman and John Arnold**

Department of Chemistry, University of California, Berkeley, California 94720, United States.

Content

A. Experimental section

General Considerations. Unless otherwise noted, all reactions were performed either using standard Schlenk line techniques or in an MBraun inert atmosphere glovebox under an atmosphere of purified nitrogen (<1 ppm O2/H2O). Glassware and cannulae were stored in an oven at ∼160 °C for at least 12 h prior to use. Hexanes, OEt_2, toluene and benzene were purified by passage through a column of activated alumina, stored over 3 or 4 Å molecular sieves, and degassed prior to use. Hexamethyldisiloxane (HMDSO) was dried over sodium/benzophenone, distilled under reduced pressure, degassed, and stored over 4 Å molecular sieves. C_6D_6 was dried over sodium/benzophenone, and $CDCl_3$ was dried over CaH_2. The deuterated solvents were then vacuum-transferred to a storage flask and degassed before being stored over activated molecular sieves in the drybox. [(BDI)(N^tBu)(Ph)Nb(F)] was prepared using literature procedure.[1] All other reagents were acquired from commercial sources and used as received. NMR spectra were recorded on Bruker AV-300, AVQ-400, AVB-400, DRX-500, AV-500, and AV-600 spectrometers. Chemical shifts were measured relative to residual solvent peaks, which were assigned relative to an external TMS standard set at 0.00 ppm. ^{19}F chemical shifts were referenced to an external standard ($BF_3.OEt_2$ set at 0.00 ppm). ^1H and ^{13}C NMR assignments were routinely confirmed by $^1H-^1H$ COSY and $^1H-^{13}C$ HSQC experiments. Samples for UV−vis NIR spectroscopy were prepared in a Schlenk-adapted quartz cuvette and analyzed on a Varian Cary 50 scanning spectrophotometer. Photo-activation reactions were conducted using a Rayonet reactor (model RPR-100) centered at 253 nm. Melting points were determined using sealed capillaries prepared under nitrogen on an Optmelt SRS. Elemental analyses were performed either at the School of Human Sciences, Science Center, London Metropolitan University or at the College of Chemistry, University of California, Berkeley. X-ray structural determinations were performed at CHEXRAY, University of California, Berkeley using a Bruker SMART APEX II QUAZAR diffractometer. Mass spectra were acquired using a Finnigan LTQ FT mass spectrometer equipped with an ESI source: THF or hexane solutions were prepared and filtered in the glovebox and maintained under a nitrogen atmosphere until injection in the spectrometer through a syringe pump. Mass spectra were recorded over a mass range (m/z) of 400-2000 with Fourier Transform Ion Cyclotron Resonance (FT-ICR) MS detector, while MS/MS data was obtained with linear ion trap (LTQ) analyzer. The exact mass and experimental isotopic profiles were compared in each case to the theoretical ones.

[(BDI)Nb(N^tBu)(Ph)(N_3)] (**1**).

TMS azide (189 µL, 1.43 mmol, 1.5 equiv.) was added to a 60 mL benzene solution of [(BDI)Nb(N^tBu)(Ph)(F)] (644 mg, 0.95 mmol, 1 equiv.) at room temperature and the reaction mixture was then heated to 60°C for 2 days. The reaction vessel was covered with aluminum foil to protect it from ambient light. The resulting yellow suspension was allowed to cool to room temperature and volatiles were removed *in vacuo*. The residue was extracted with the minimum volume of OEt_2 and stored at -40°C in absence of light, affording

---

[1] Gianetti, T. L.; Bergman, R. G.; Arnold, J. *Chem. Sci.* **2014**, *5*, 2517–2524.

yellow crystals of **1** (530 mg, 0.756 mmol, 80% yield). Yellow single crystals suitable for X-ray diffraction were obtained from a concentrated Et_2O solution stored at room temperature for 12h. ^1H NMR (500 MHz, $CD_3C_6D_5$, 250K) δ = 8.27 (br s, 1H, Nb-C_6H_5), 7.75 (br s, 1H, Nb-C_6H_5), 6.95 – 7.15 (m, 9H, CH_{Ar}), 5.29 (s, 1H, *H*C(C(Me)NAr))(C(CH_2)NAr), 3.05 (sept, *J* = 6.2 Hz, 1H, C*H*Me_2), 2.83 (sept, *J* = 6.5 Hz, 2H, C*H*Me_2), 2.75 (sept, *J* = 6.4 Hz, 1H, C*H*Me_2), 1.53 (s, 3H, ArNC*Me*), 1.44 (s, 3H, ArNC*Me*), 1.41 (m, 6H, CH*Me*$_2$), 1.11 (d, *J* = 6.8 Hz, 3H, CH*Me*$_2$), 1.09 (d, *J* = 6.8 Hz, 3H, CH*Me*$_2$), 1.05 (s, 9H, N^t*Bu*), 1.03 (m, 9H, CH*Me*$_2$), 0.66 (d, *J* = 6.4 Hz, 3H, CH*Me*$_2$). ^1H NMR (500 MHz, $CD_3C_6D_5$, 350K) δ = 7.96 (br s, 2H, Nb-C_6H_5), 6.96 – 7.12 (m, 9H, CH_{Ar}), 5.51 (s, 1H, *H*C(C(Me)NAr))(C(CH_2)NAr), 2.87 (m, 4H, C*H*Me_2), 1.62 (s, 6H, ArNC*Me*), 1.03 - 1.08 (m, 24H, CH*Me*$_2$), 1.00 (s, 9H, N^t*Bu*). FT-IR (cm^{-1}) 2864(w), 2093 (s, νN_3), 1553 (s), 1504 (s), 1436 (s), 1372 (s), 1315 (m), 1229 (s), 1164 (m), 1099 (m), 1053 (m), 1020 (m), 933 (m), 855 (s), 794 (s), 759 (s), 726 (s), 697 (s). UV-vis (OEt_2): λ_1 = 302 nm (ε = 14600 $L.cm^{-1}.mol^{-1}$); λ_2 = 405 nm (ε = 4800 $L.cm^{-1}.mol^{-1}$). Anal. calcd for $C_{39}H_{55}N_6Nb$: C, 66.84; H, 7.91; N, 11.99. Found: C, 66.73; H, 7.77; N, 11.90. mp (decomp.) 140-142 °C.

[(BDI$^\#$)Nb(N^{t}Bu)(Ph)] (**2**) and {[(BDI)Nb(Ph)]$_2$(μ-N)$_2$} (**3**).

A 10 mL benzene solution of [(BDI)Nb(N^{t}Bu)(Ph)(N_3)] (**1**) (500 mg, 0.713 mmol) was irradiated in a quartz reactor for 24 hours. The color quickly turned from yellow to dark brown and a crystalline material formed. The solids were recovered by filtration, washed with 2 x 1 mL C_6H_6 and the residual solvent removed *in vacuo* to give **3** as a dark greenish-brown solid (99 mg, 0.082 mmol, 23 % yield). Single crystals of **3** suitable for X-ray diffraction were directly collected from the benzene reaction mixture. The benzene filtrate was evaporated to dryness, extracted with 2 mL HMDSO and cooled to -40°C. This produced yellow crystals of **2** that were recovered and dried *in vacuo* (118 mg, 0.179 mmol, 25 % yield). The moderate yield for **2** is due to the very high solubility of this compound in apolar solvents. Yellow single crystals of **2** suitable for X-ray diffraction were obtained upon cooling a saturated HMDSO solution of **2** to -40°C. The efficiency of the photo-degradation of complex **1** was monitored by recording ^1H NMR data on the same NMR tube before and after photo exposure. The measured conversion rate for **1** to **2** was 47%, **2** being the foremost compound observed in the crude reaction solution by ^1H NMR. Data for **2**: ^1H NMR (600 MHz, C_6D_6, 293K) δ = 8.51 (dd, *J* = 7.7, 1.3 Hz, 2H, Nb-$C_6H_{5\text{-}o}$), 7.36 (t, *J* = 7.6 Hz, 2H, Nb-$C_6H_{5\text{-}m}$), 7.33 – 7.28 (tt, *J* = 7.7, 1.3 Hz, 1H, Nb-$C_6H_{5\text{-}p}$), 7.24 (dd, *J* = 7.7, 1.5 Hz, 1H, CH_{Ar}), 7.18 (d, *J* = 7.6 Hz, 1H, CH_{Ar}), 7.10 (dd, *J* = 7.6, 1.5 Hz, 1H, CH_{Ar}), 7.08 – 7.04 (m, 2H, CH_{Ar}), 6.99 (dd, *J* = 6.9, 2.3 Hz, 1H, CH_{Ar}), 5.64 (s, 1H, *H*C(C(Me)NAr))(C(CH_2)NAr), 3.92 (s, 1H, C(C*H*$_2$)NAr), 3.75 (sept, *J* = 6.8 Hz, 1H, C*H*Me_2), 3.64 (sept, *J* = 6.8 Hz, 1H, C*H*Me_2), 3.44 (s, 1H, C(C*H*$_2$)NAr), 3.06 (sept, *J* = 6.8 Hz, 1H, C*H*Me_2), 2.93 (sept, *J* = 6.8 Hz, 1H, C*H*Me_2), 1.51 (d, *J* = 6.8 Hz, 3H, CH*Me*$_2$), 1.50 (d, *J* = 6.8 Hz, 3H, CH*Me*$_2$), 1.48 (s, 3H, ArNC*Me*), 1.40 (d, *J* = 6.9 Hz, 3H, CH*Me*$_2$), 1.29 (d, *J* = 6.8 Hz, 3H, CH*Me*$_2$), 1.23 (d, *J* = 6.8 Hz, 3H, CH*Me*$_2$), 1.09 (d, *J* = 6.8 Hz, 3H, CH*Me*$_2$), 1.00 (s, 9H, N^t*Bu*), 0.99 (d, *J* = 6.8 Hz, 3H, CH*Me*$_2$), 0.78 (d, *J* = 6.7 Hz, 3H). $^{13}C\{^1H\}$ NMR (125.8 MHz, $CDCl_3$, 293K) δ = 149.18 (C, N*C*(CH_3)=C), 145.77 (C, Ar), 145.73 (C, Ar), 143.73 (C, Ar), 143.68 (C, Ar), 143.27 (C, Ar), 143.09 (C, Ar), 142.57 (C, Ar), 136.26 (CH, Nb-*C*$_6H_{5\text{-}o}$), 129.98 (CH, Nb-*C*$_6H_{5\text{-}p}$), 127.09 (CH, Ar), 126.95 (CH, Ar), 126.79 (CH, Nb-*C*$_6H_{5\text{-}m}$), 124.45 (CH, Ar), 123.89 (CH, Ar), 123.87 (CH, Ar), 123.85 (CH, Ar), 101.09 (CH, H*C*(=C(Me))(C(CH_2)), 100.37 (C, N*C*(=CH_2)), 88.26 (CH_2, NC(=*C*H$_2$)), 70.81 (C, *C*(Me)$_3$), 32.04 (CH_3, Nb=N^t*Bu*), 29.67 (CH, ^{i}Pr), 28.86 (CH, ^{i}Pr), 28.84 (CH, ^{i}Pr), 28.61 (CH, ^{i}Pr), 25.77 (CH_3, ^{i}Pr), 25.60 (CH_3, ^{i}Pr), 25.54 (CH_3, ^{i}Pr), 25.21 (CH_3, ^{i}Pr), 24.94 (CH_3, ^{i}Pr), 24.66 (CH_3, ^{i}Pr), 24.14 (CH_3, ^{i}Pr), 23.99 (CH_3, ^{i}Pr), 22.65 (CH_3, HC(C(*Me*)NAr)$_2$). FT-IR (cm^{-1}) 3102(w), 3053 (m), 2923 (s), 2854 (s), 1598 (m), 1552 (m), 1520 (m), 1463 (s), 1438 (s), 1377 (s), 1324 (sw), 1292 (m), 1252 (s), 1235 (s), 1211 (m), 1107 (m), 1062 (m), 1001 (s), 932 (w), 855 (w), 823 (w), 797 (s), 770 (m), 754 (w), 727 (m), 701 (m), 654 (w). Anal. calcd for $C_{39}H_{54}N_3Nb$: C, 71.21; H, 8.28; N, 6.39. Found: C, 71.03; H, 8.99; N, 6.42. mp: (decomp) 142-145 °C.

Data for **3**: Complex **3** is insoluble in hydrocarbon solvents. In $CDCl_3$, complex **3** decomposes within seconds, the solution turning from dark green to dark brown. This precluded NMR analysis of this compound. FT-IR (cm^{-1}) 2921 (s), 2853 (s), 1533 (m), 1462 (s), 1378 (s), 1312 (m), 1250 (m), 1168 (w), 1095 (w), 1056 (w), 1021 (m), 927 (w), 864 (w), 845 (w), 791 (m), 760 (m), 721 (m), 697 (w), 677 (m), 516 (w). ES-MS (THF) : m/z= 1203.5587 [M+H]$^+$ (Calcd for $C_{70}H_{93}N_6Nb_2$: 1203.5589). Anal. calcd for $C_{70}H_{92}N_6Nb_2$.(C_6H_6): C, 71.23; H, 7.71; N, 6.56. Found: C, 71.05; H, 8.17; N, 6.65. mp: (decomp) 153-155 °C.

[(BDI)Nb(N^{t}Bu)(Ph)($N_3B(C_6F_5)_3$)] (**4**).

$B(C_6F_5)_3$ (146 mg, 0.256 mmol, 1 equiv.) was added to a 20 mL toluene solution of **1** (200 mg, 0.256 mmol, 1 equiv.). The reaction mixture was stirred for 12 hours at room temperature, and turned from yellow to orange. The reaction vessel was covered with aluminum foil to protect it from ambient light. The volatiles were removed *in vacuo* and the residue was then extracted with Et_2O to give an orange solution that was filtered, concentrated and stored at -40°C overnight. This afforded orange crystals of **4** (197 mg, 0.162 mmol, 63%). Single crystals suitable for X-ray diffraction were obtained similarly. ^{1}H NMR (500 MHz, $CD_3C_6D_5$, 250K) δ = 8.33 (d, *J* = 7.0 Hz, 1H, CH_{Ar}), 7.58 (d, *J* = 7.0 Hz, 1H, CH_{Ar}), 7.41 (t, *J* = 7.4 Hz, 1H, CH_{Ar}), 7.21 (d, *J* = 7.1 Hz, 1H, CH_{Ar}), 6.94 - 7.09 (m, 5H, CH_{Ar}), 6.79 (d, *J* = 7.5 Hz, 1H, CH_{Ar}), 6.72 (d, *J* = 7.6 Hz, 1H, CH_{Ar}), 4.97 (s, 1H, *H*C(C(Me)NAr))(C(CH_2)NAr), 2.66 (sept, *J* = 6.2 Hz, 1H, C*H*Me$_2$), 2.44 (sept, *J* = 6.1 Hz, 1H, C*H*Me$_2$), 2.32 (sept, *J* = 6.4 Hz, 2H, C*H*Me$_2$), 1.31 (d, *J* = 5.8 Hz, 3H, CH*Me*$_2$), 1.21 (s, 3H, ArNC*Me*), 1.19 (d, *J* = 6.1 Hz, 3H, CH*Me*$_2$), 1.15 (s, 3H, ArNC*Me*), 0.93 (m, 6H, CH*Me*$_2$), 0.80 (d, *J* = 6.2 Hz, 3H, CH*Me*$_2$), 0.77 (d, *J* = 6.5 Hz, 3H, CH*Me*$_2$), 0.72 (d, *J* = 5.8 Hz, 3H, CH*Me*$_2$), 0.58 (s, 9H, N^t*Bu*), 0.44 (d, *J* = 5.7 Hz, 3H, CH*Me*$_2$). ^{1}H NMR (500 MHz, $CD_3C_6D_5$, 350K) δ = 8.01 (br s, 2H, CH_{Ar}), 7.18 (br s, 3H, CH_{Ar}), 6.99 – 7.09 (m, 6H, CH_{Ar}), 5.56 (s, 1H, *H*C(C(Me)NAr))(C(CH_2)NAr), 2.55 - 2.69 (br m, 4H, C*H*Me$_2$), 1.56 (s, 6H, ArNC*Me*), 1.32 (br s, 6H, CH*Me*$_2$), 0.95 (br s, 12H, CH*Me*$_2$), 0.77 (s, 9H, N^t*Bu*), 0.68 (br s, 6H, CH*Me*$_2$). ^{19}F NMR (376 MHz, THF-*d*$_8$, 293 K) δ(ppm) −132, −156, and −163 ($B(C_6F_5)_4$). FT-IR (cm^{-1}) 2902 (s), 2853 (s), 2181 (s, νN_3), 1645 (w), 1514 (w), 1468 (s), 1378 (s), 1315 (w), 1285 (w), 1230 (w), 1100 (m), 977 (m), 860 (w), 796 (m), 727 (w). UV-vis (OEt_2) λ_1 = 311 nm (ε = 26900 L.cm^{-1}.mol^{-1}), λ_2 = 389 nm (ε = 7500 L.cm^{-1}.mol^{-1}). Anal. calcd for $C_{57}H_{55}F_{15}BN_6Nb$: C, 56.45; H, 4.57; N, 6.93. Found: C, 56.45; H, 4.70; N, 6.84. mp (decomp.): 144-146 °C.

[(BDI)Nb(N(Ph)^{t}Bu)(NB(C_6F_5)$_3$)] (**5**).

A bright orange toluene (20 mL) solution of compound **4** (107 mg, 0.088 mmol) was introduced in a quartz shlenk reaction vessel and the reaction mixture was photolyzed for 12 hours at room temperature. The color turned a lighter shade of orange. The volatiles were removed in vacuo and the residue was extracted with Et_2O to give an orange solution that was concentrated, filtered and stored at -40°C overnight. This produced yellow crystals of **5** that were collected and dried *in vacuo* (70 mg, 0.059 mmol, 67%). Yellow single crystals suitable for X-ray diffraction were obtained similarly. ^1H NMR (400 MHz, C_6D_6, 293K) δ = 7.22 (t, *J* = 7.8 Hz, 2H, CH_{Ar}), 7.04 (d, *J* = 8.0 Hz, 4H, CH_{Ar}), 6.66 – 6.77 (m, 5H, CH_{Ar}), 4.25 (s, 1H, *H*C(C(Me)NAr))(C(CH_2)NAr), 3.00 (sept, *J* = 6.7 Hz, 2H, C*H*Me_2), 2.31 (sept, *J* = 6.6 Hz, 2H, C*H*Me_2), 3.44 (s, 1H, C(C*H*$_2$)NAr), 1.37 (s, 9H, N^t*Bu*), 1.33 (d, *J* = 6.6 Hz, 6H, CH*Me*$_2$), 1.14 (s, 6H, ArNC*Me*), 1.10 (d, *J* = 6.7 Hz, 6H, CH*Me*$_2$), 0.99 (d, *J* = 6.5 Hz, 3H, CH*Me*$_2$), 0.77 (d, *J* = 6.7 Hz, 3H, CH*Me*$_2$). $^{13}C\{^1H\}$ NMR (125.8 MHz, C_6D_6, 293K) δ = 170.6 (C, HC(*C*(Me)NAr)$_2$), 144.2 (C, Ar), 144.0 (C, Ar), 141.9 (C, Ar), 140.6 (C, Ar), 132.3 (CH, Ar), 128.8 (CH, Ar), 125.8 (CH, Ar), 124.8 (CH, Ar), 102.5 (CH, H*C*(C(Me)NAr)$_2$), 31.6 (CH_3, Nb=N^t*Bu*), 29.1 (CH, ^{i}Pr), 28.5 (CH, ^{i}Pr), 26.6 (CH_3, ^{i}Pr), 26.2 (CH_3, HC(C(*Me*)NAr)$_2$), 25.1 (CH_3, ^{i}Pr), 24.7 (CH_3, ^{i}Pr), 24.4 (CH_3, ^{i}Pr). ^{19}F NMR (376 MHz, THF-d_8, 293 K) δ(ppm) −129, −160, and −163 ($B(C_6F_5)_4$). FT-IR (cm^{-1}) 2956 (s), 2923 (s), 2853 (s), 1640 (w), 1513 (w), 1462 (s), 1378 (m), 1260 (m), 1178 (w), 1096 (m), 1017 (m), 798 (m). Anal. calcd for $C_{57}H_{55}F_{15}BN_4Nb$: C, 57.78; H, 4.68; N, 4.73. Found: C, 57.75; H, 4.66; N, 4.58. mp: (decomp) 164-166 °C.

Reaction of **5** with $[Me_4N]F$.

Scheme 1. Synthesis of complex 6. Ar = 2,6-diisopropylphenyl.

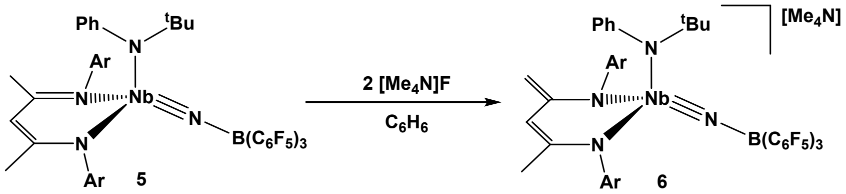

$[Me_4N]F$ (8.7 mg, 0.093 mmol, 2 equiv.) was added to a 10 mL toluene solution of **5** (55.3 mg, 0.047 mmol, 1 equiv.). The reaction mixture turned a lighter shade of yellow. The reaction was stirred at room temperature for 15h. The volatiles were removed *in vacuo* and the yellow residue was extracted into Et_2O, filtered, concentrated and stored at -40°C overnight. This produced yellow crystals of $[NMe_4][(BDI^{\#})Nb(N(Ph)^tBu)(NB(C_6F_5)_3)]$ (**6**) (22 mg, 0.018 mmol, 39% yield). Single crystals of **6** suitable for X-ray diffraction were grown from a saturated benzene solution at r.t.; the solid-state structure for **6** is presented in the following section. The ^1H NMR spectrum for **6** shows signals in agreement with deprotonated BDI ligand, notably two resonances centered at 3.71 and 3.07 ppm corresponding to the two inequivalent protons of the β-methylene group. ^1H NMR (600 MHz, C_6D_6, 293K) δ = 7.74 (d, 1H, C*H*$_{Ar}$), 7.51 (d, 1H, C*H*$_{Ar}$), 7.43 (t, 1H, C*H*$_{Ar}$), 7.35 (m, 2H, C*H*$_{Ar}$), 7.24 (d, 1H, C*H*$_{Ar}$), 7.09 (d, 1H, C*H*$_{Ar}$), 7.02 (m, 1H, C*H*$_{Ar}$), 6.95 (s, 1H, C*H*$_{Ar}$), 4.74 (s, 1H, *H*C(C(Me)NAr))(C(CH_2)NAr), 4.24 (sept, J = 6.8 Hz, 1H, C*H*Me_2), 4.00 (sept, J =

6.8 Hz, 1H, C*H*Me$_2$), 3.89 (m, 1H, C*H*Me$_2$), 3.71 (s, 1H, C(C*H$_2$*)NAr), 3.07 (s, 1H, C(C*H$_2$*)NAr), 1.78 (d, J = 6.8 Hz, 3H, CH*Me$_2$*), 1.68 (d, J = 6.8 Hz, 3H, CH*Me$_2$*), 1.66 (s, 3H, C(C*H$_3$*)NAr), 1.59 (d, J = 6.8 Hz, 3H, CH*Me$_2$*), 1.47 (s, 9H, N^t*Bu*), 1.41-0.99 (m, 16H, CH*Me$_2$*). Anal. calcd for $C_{61}H_{66}F_{15}BN_5Nb$: C, 58.28; H, 5.29; N, 5.57. Found: C, 57.90; H, 5.10; N, 5.02.

B. NMR and IR spectroscopic data

Figure S1. ^{1}H NMR monitoring of the reaction between (BDI)Nb(N^{t}Bu)(Ph)F and TMS-N$_3$ (C_6D_6, 293K, 400MHz).

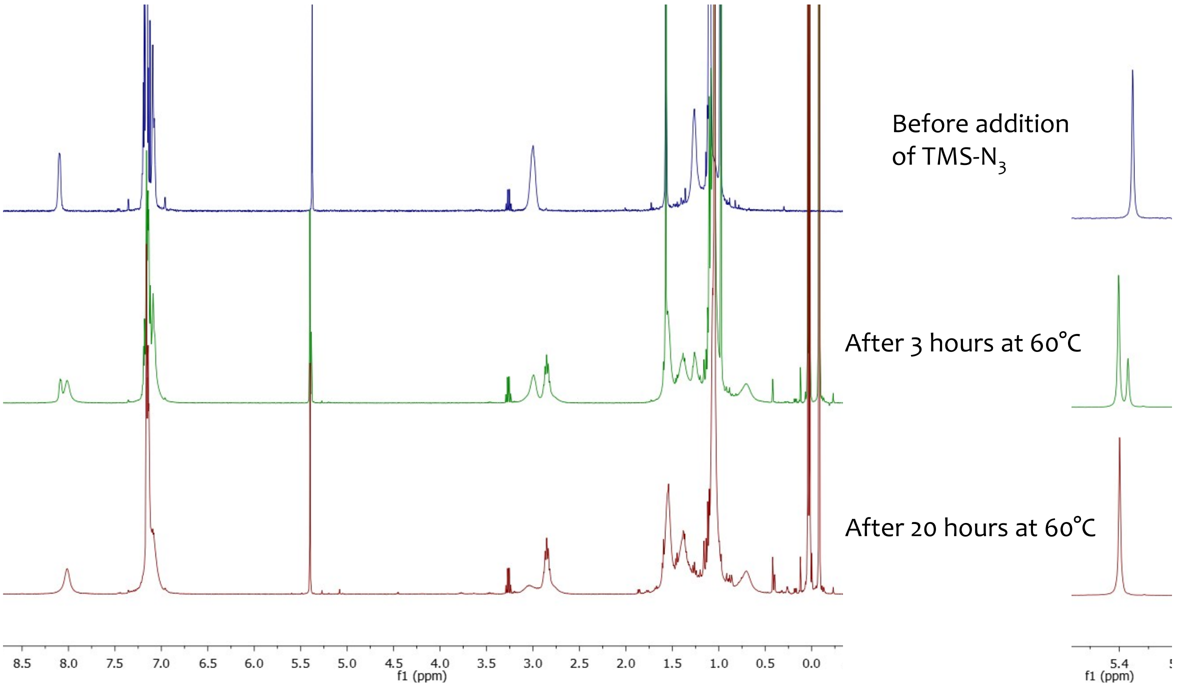

Figure S2. ^{19}F NMR spectrum of the crude reaction mixture between (BDI)Nb(N^{t}Bu)(Ph)F and TMS-N$_3$ after 20 h at 60°C showing the characteristic resonance for TMS-F (C_6D_6, 293K, 400MHz).

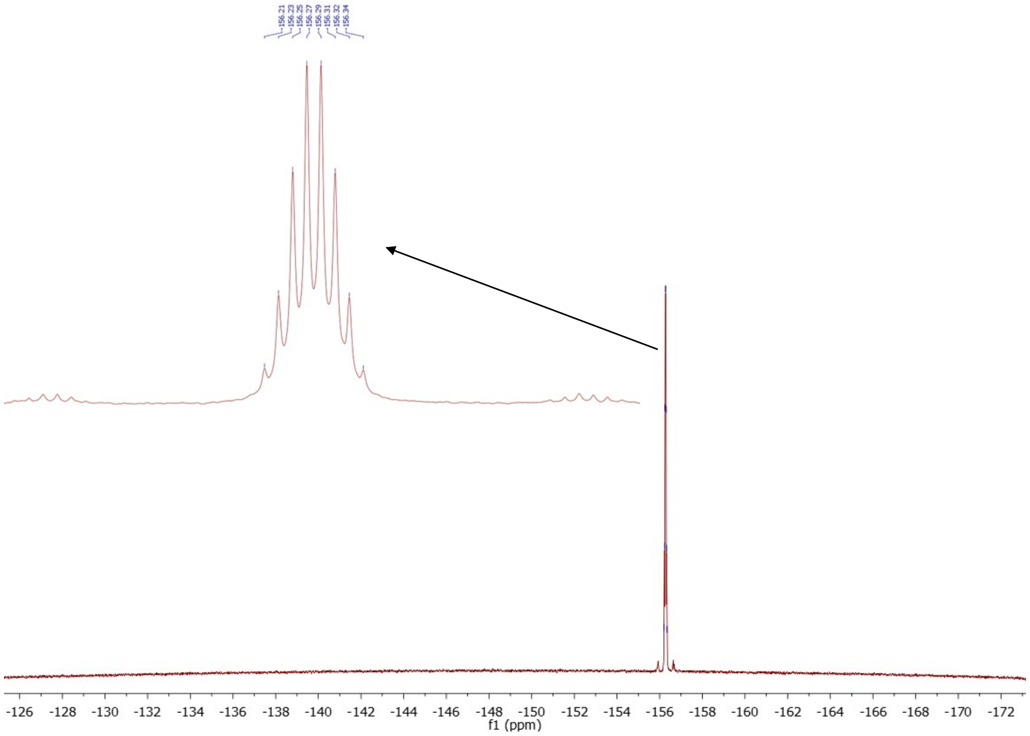

Figure S3. ^{1}H NMR spectrum for **1** (C_7D_8, 250K, 500MHz).

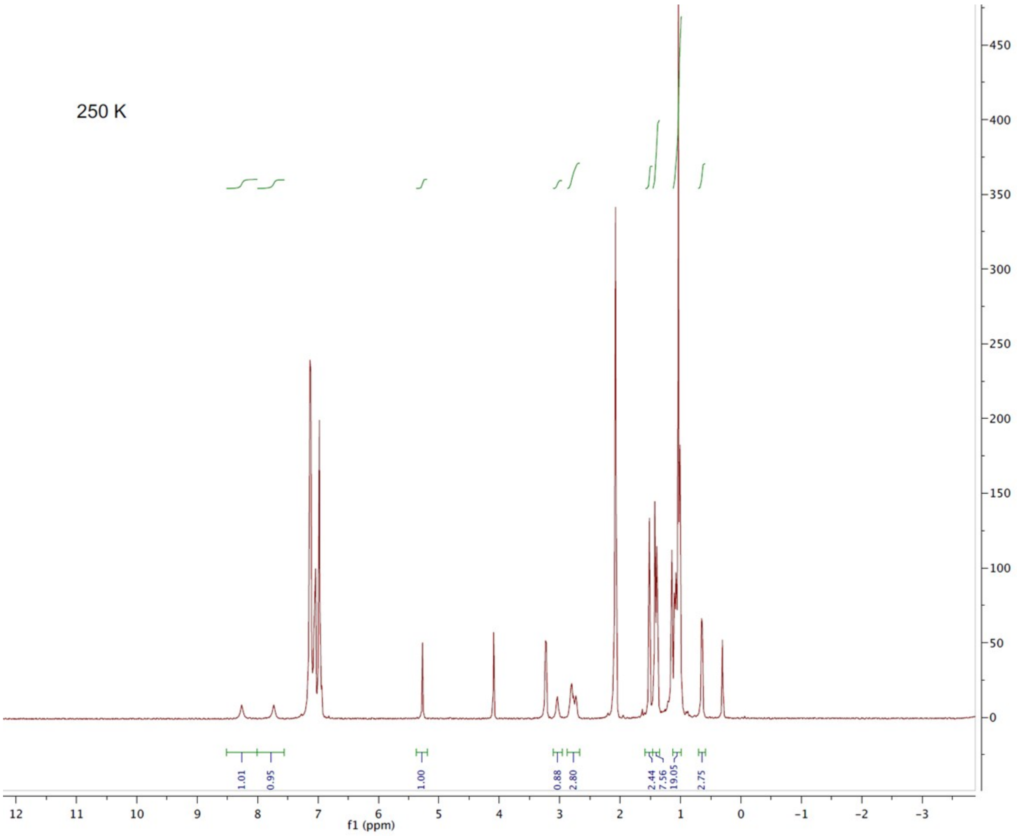

Figure S4. Variable temperature (250-350 K) ^{1}H NMR spectrum for **1** (C_7D_8, 500MHz).

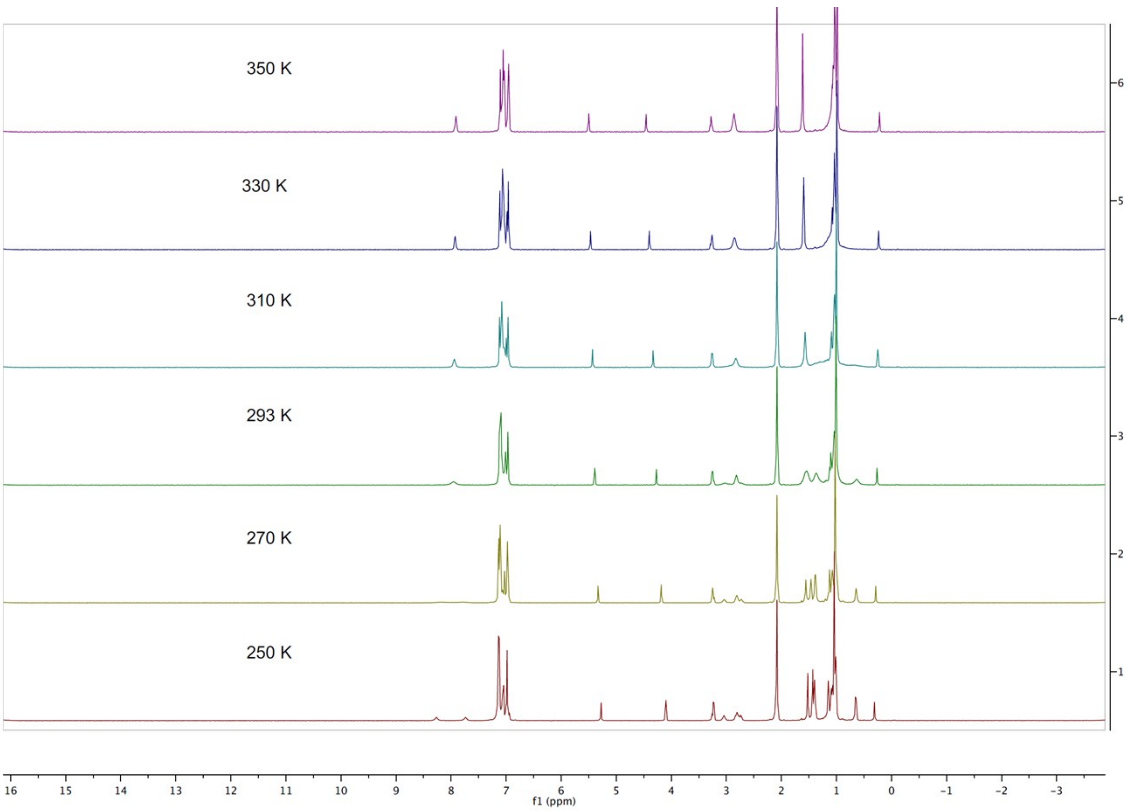

Figure S5. IR spectrum for **1**.

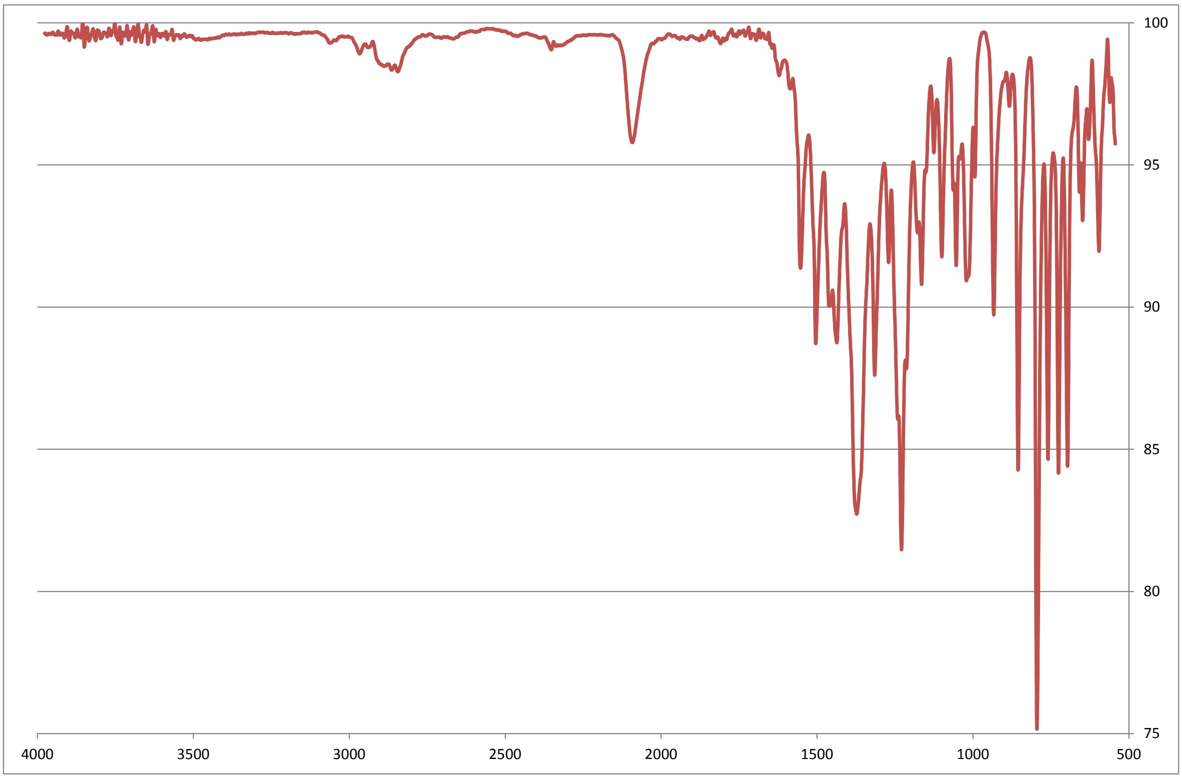

Figure S6. ^{1}H NMR spectrum of the crude reaction mixture after photolysis of **1** (C_6D_6, 293K, 400MHz).

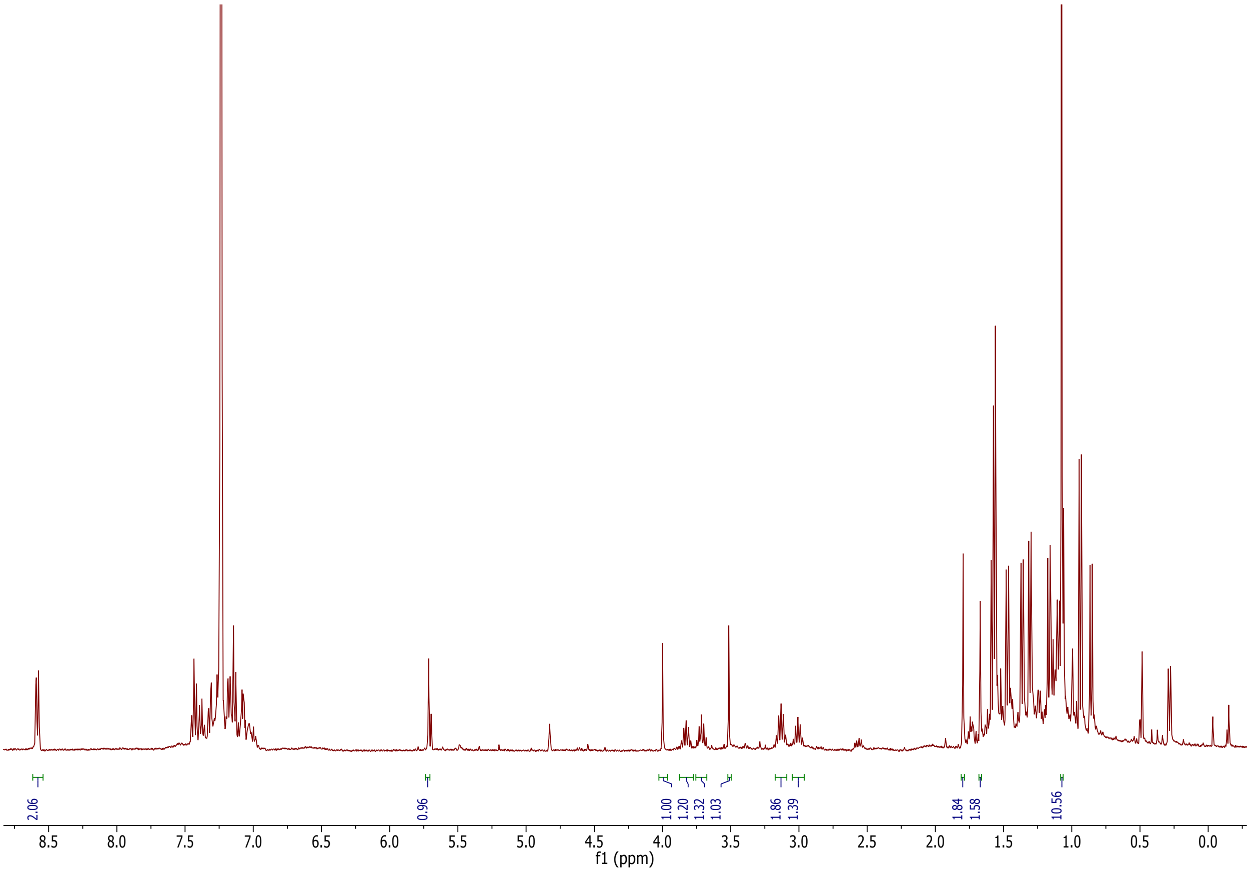

Figure S6-bis. ^{1}H NMR spectrum for **2** (C_6D_6, 293K, 600MHz).

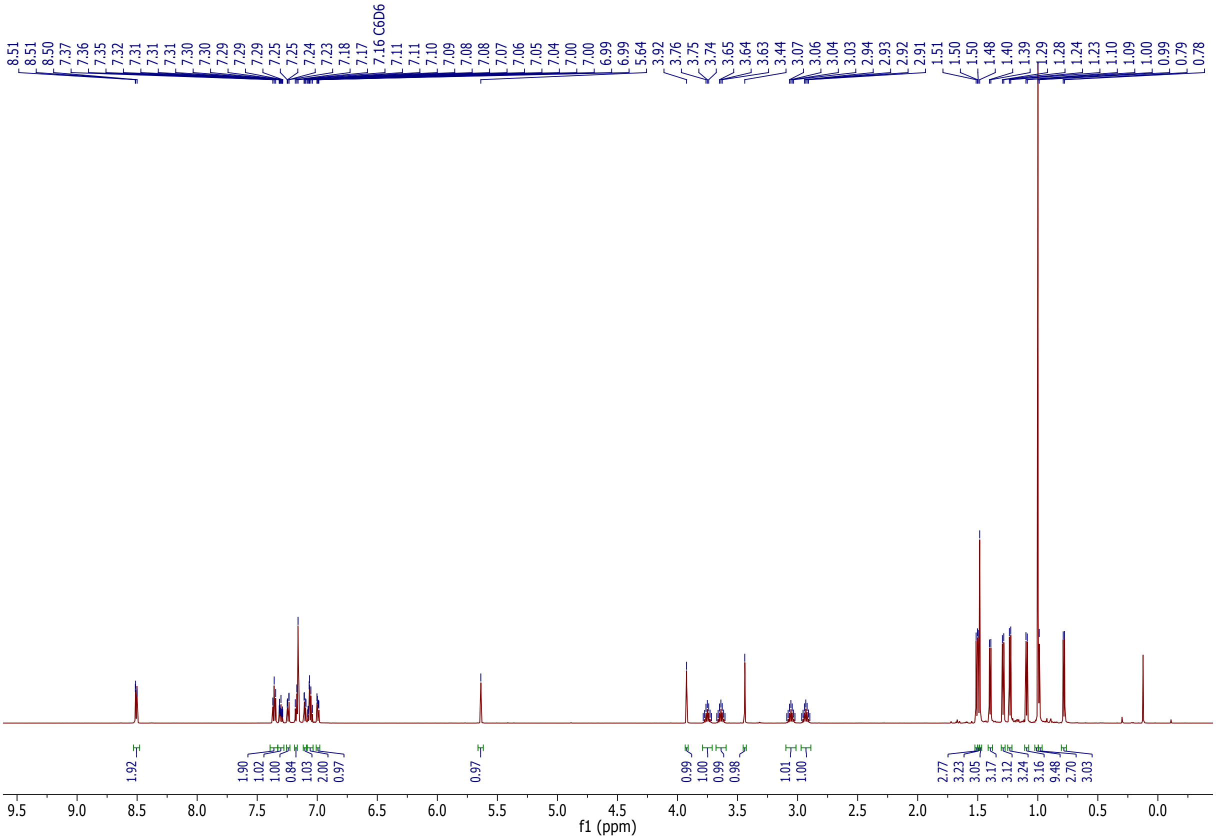

Figure S7. ^{1}H-^{1}H COSY NMR spectrum for **2** (C_6D_6, 293K, 600MHz).

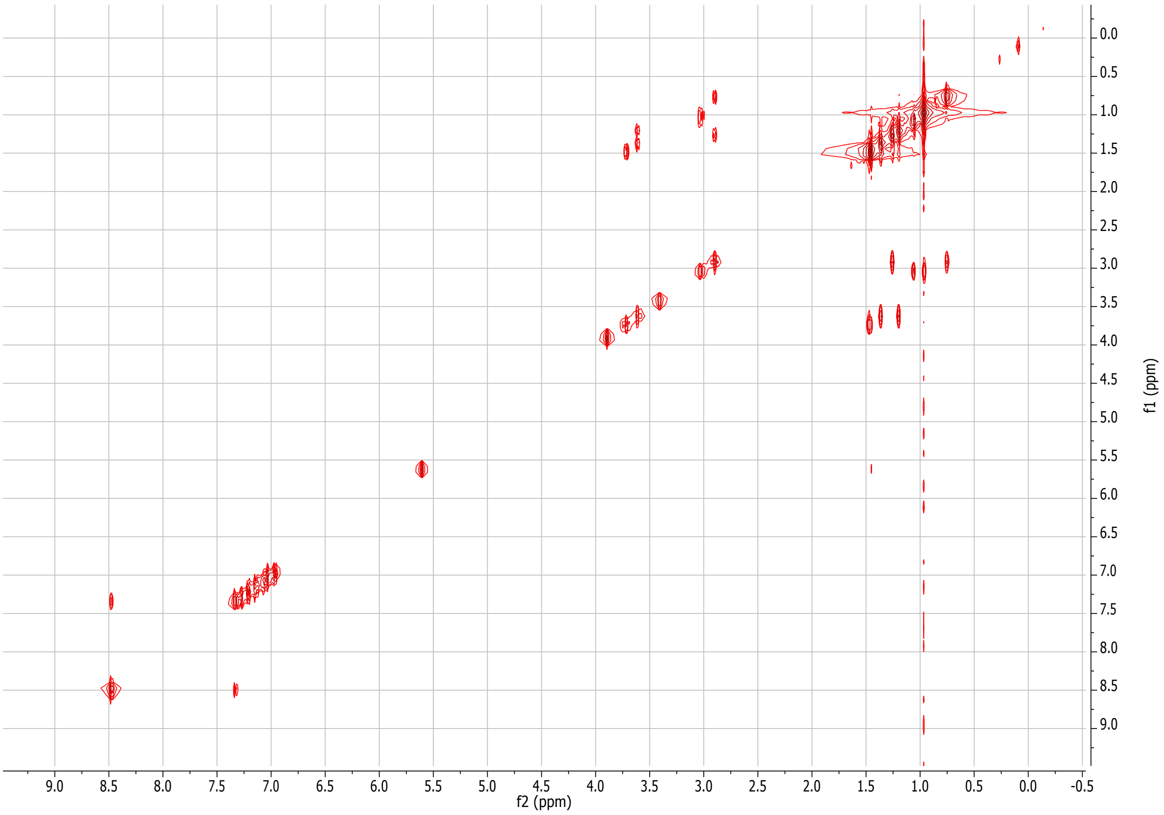

Figure S8. ^{1}H-^{13}C HSQC NMR spectrum for **2** (C_6D_6, 293K, 600MHz).

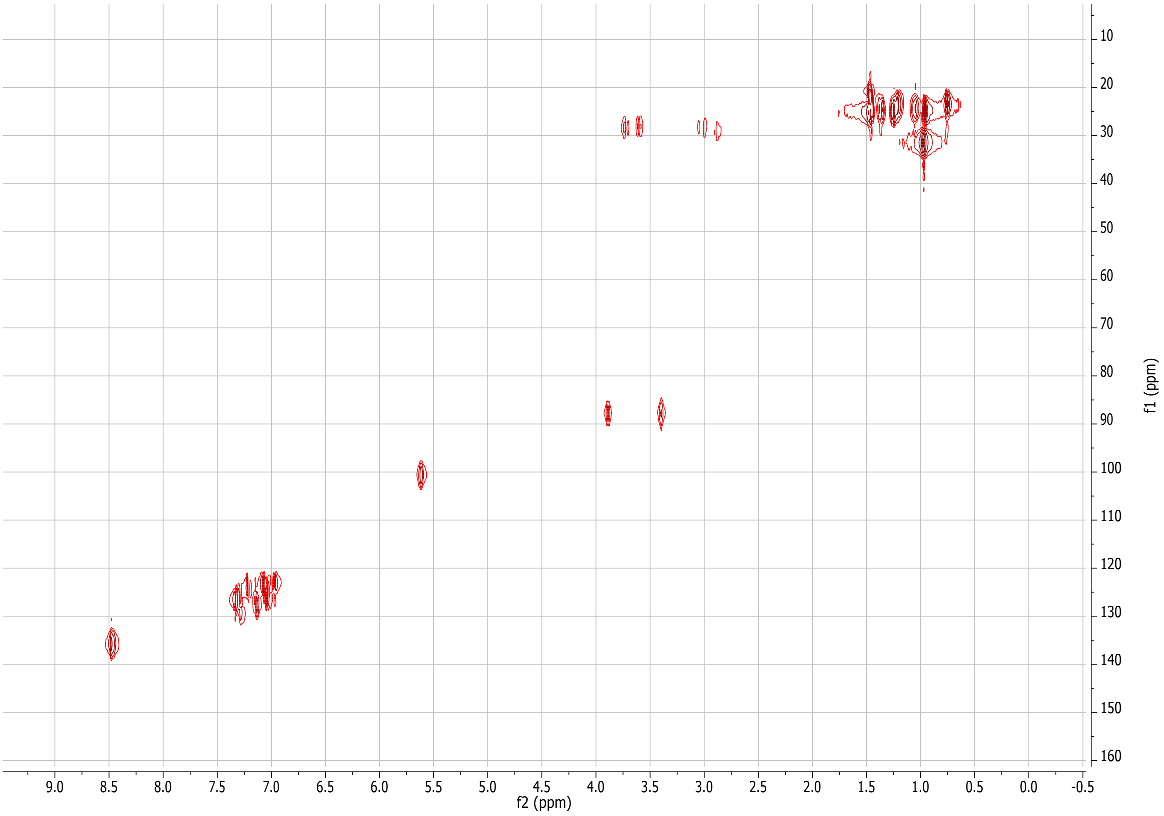

Figure S9. IR spectrum for **2**.

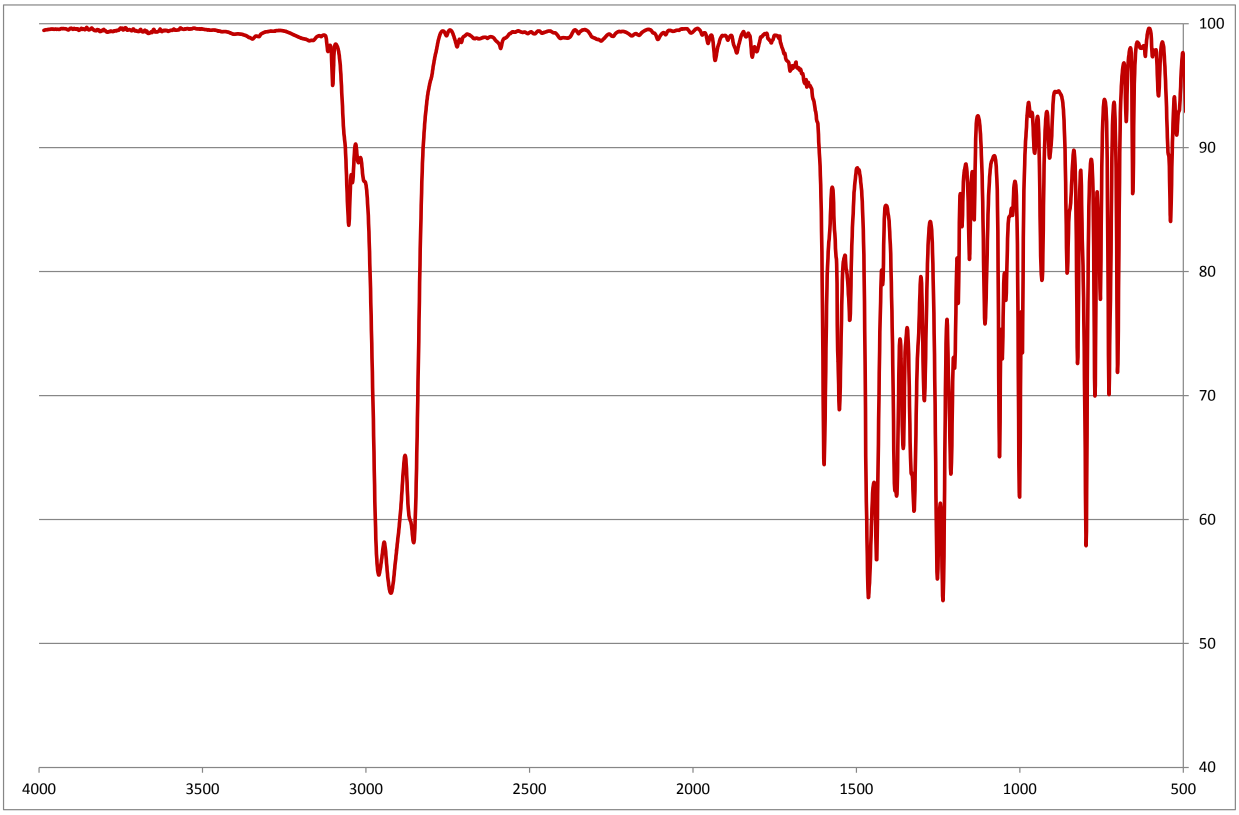

Figure S10. IR spectrum for **3**.

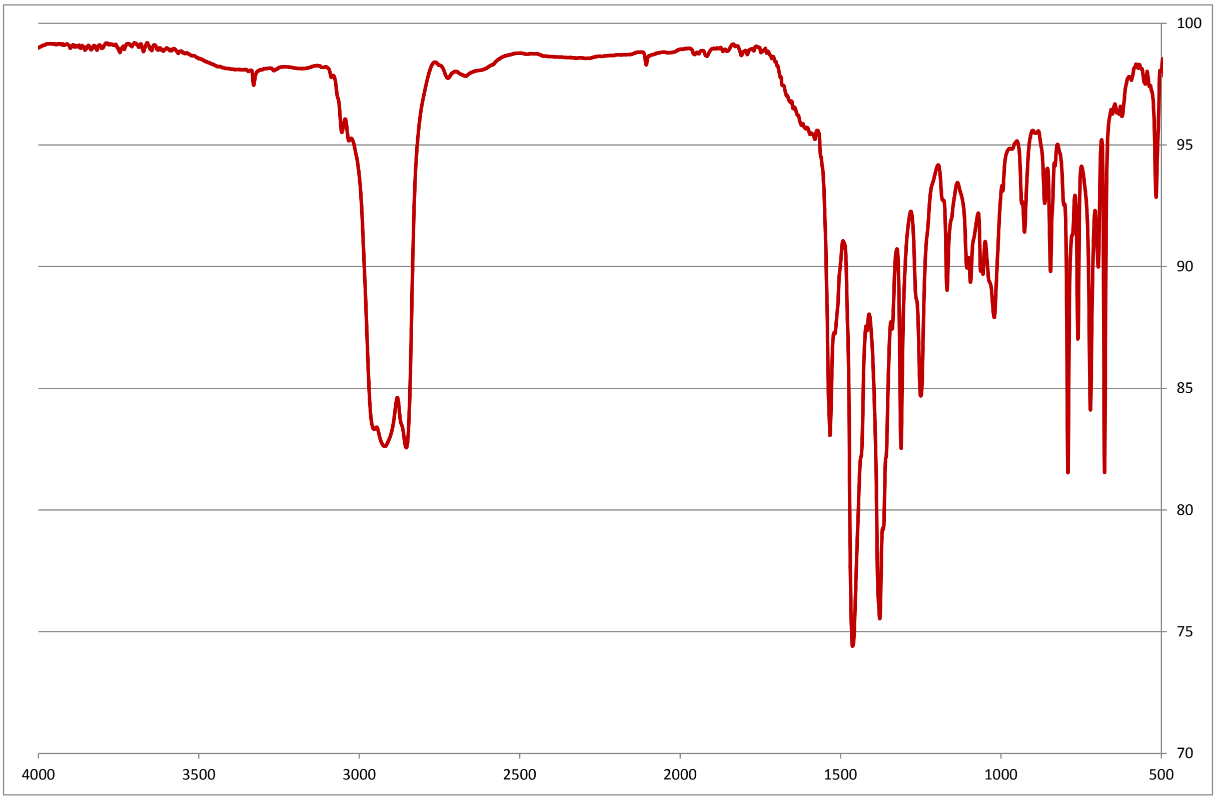

Figure S11. Variable temperature (230-350 K) ^{1}H NMR spectrum for **4** (C_6D_6, 500MHz).

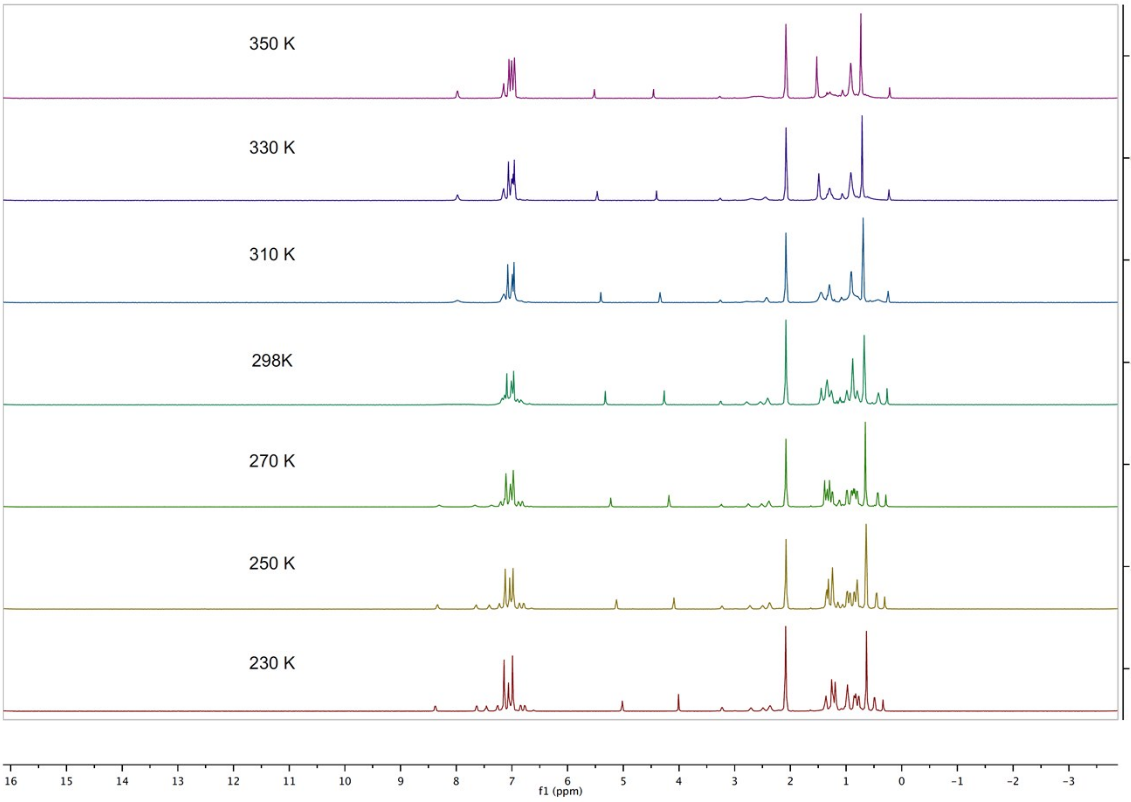

Figure S12. ^{19}F NMR spectrum for **4** (376 MHz, THF-d_8, 293 K).

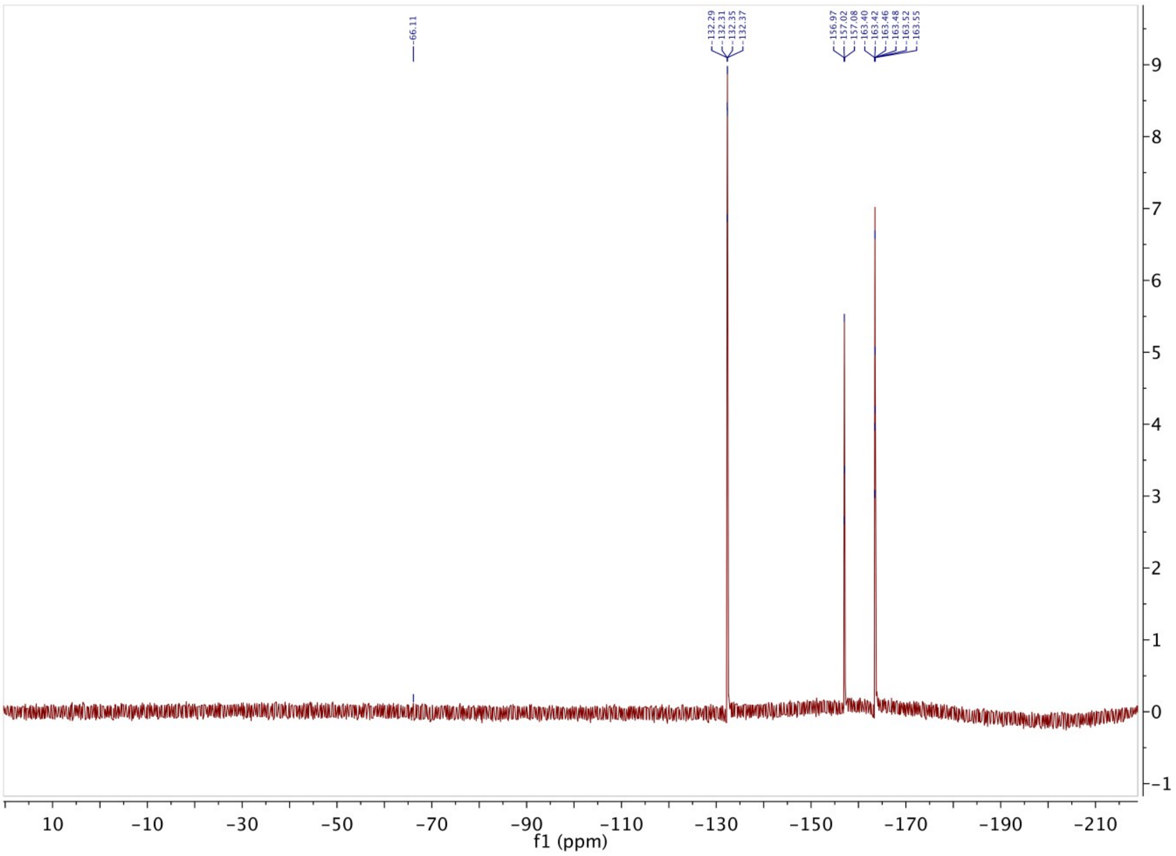

Figure S13. IR spectrum for **4**.

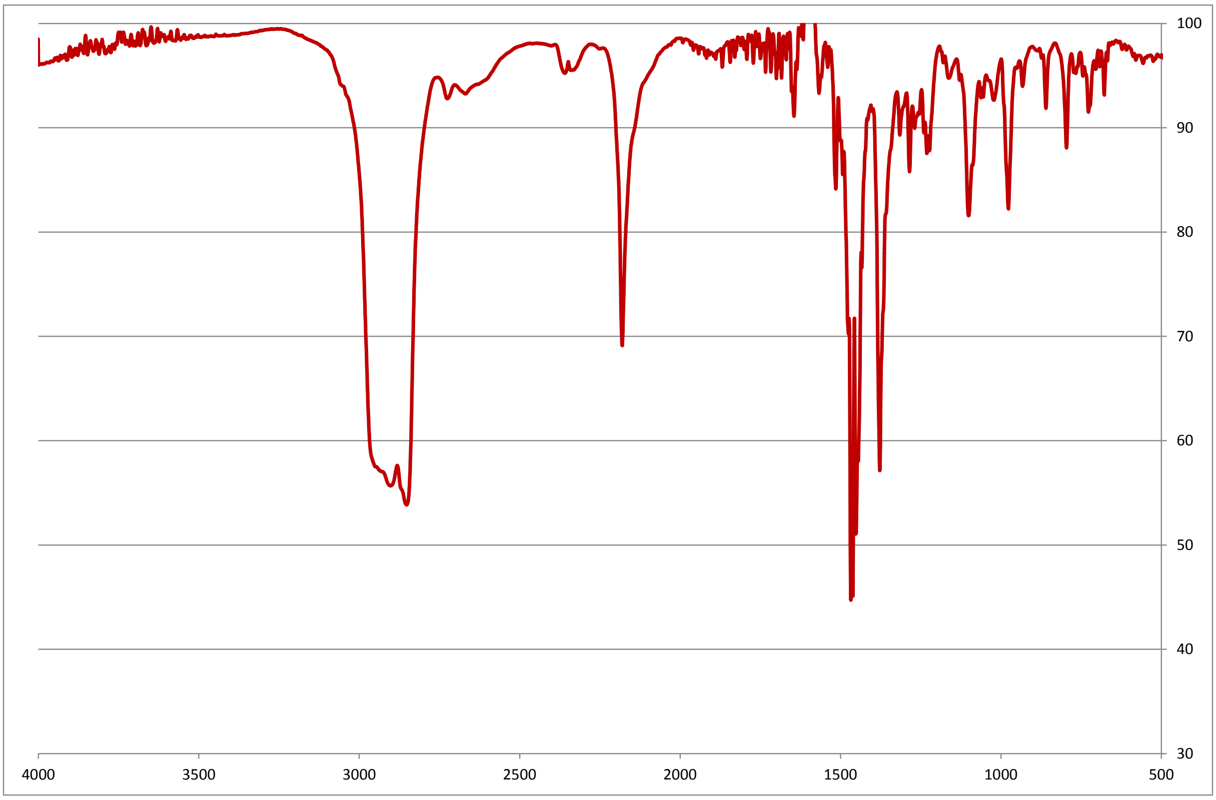

Figure S14. ^{1}H NMR spectrum for **5** (C_6D_6, 293K, 400MHz).

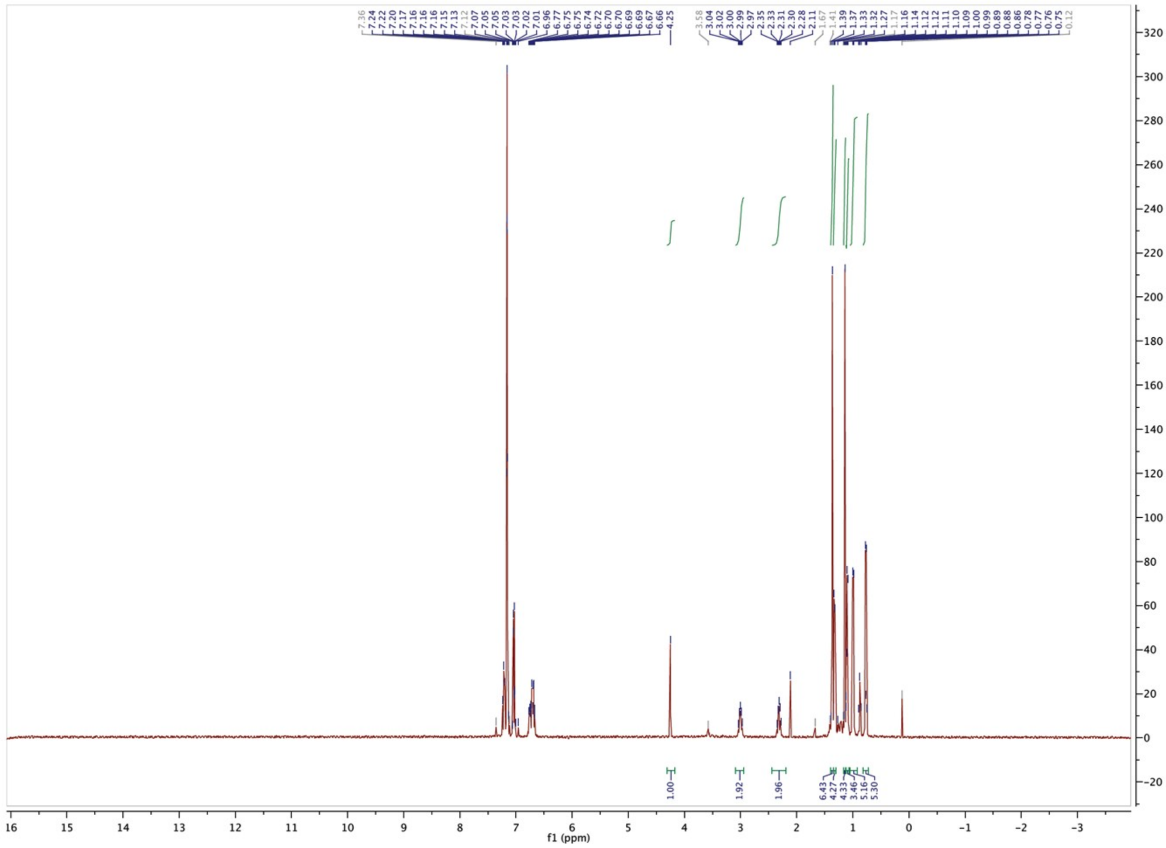

Figure S15. ^{19}F NMR spectrum for **5** (376 MHz, THF-d_8, 293 K).

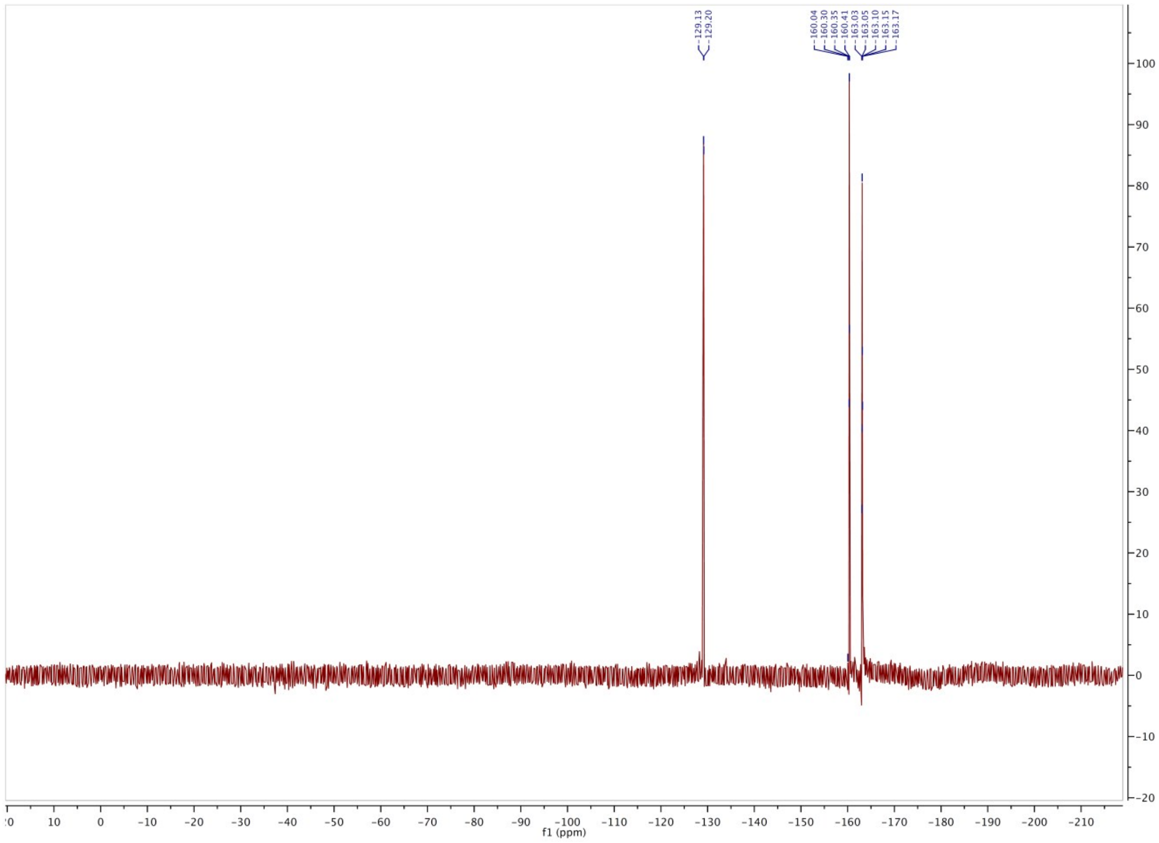

Figure S16. IR spectrum for **5**.

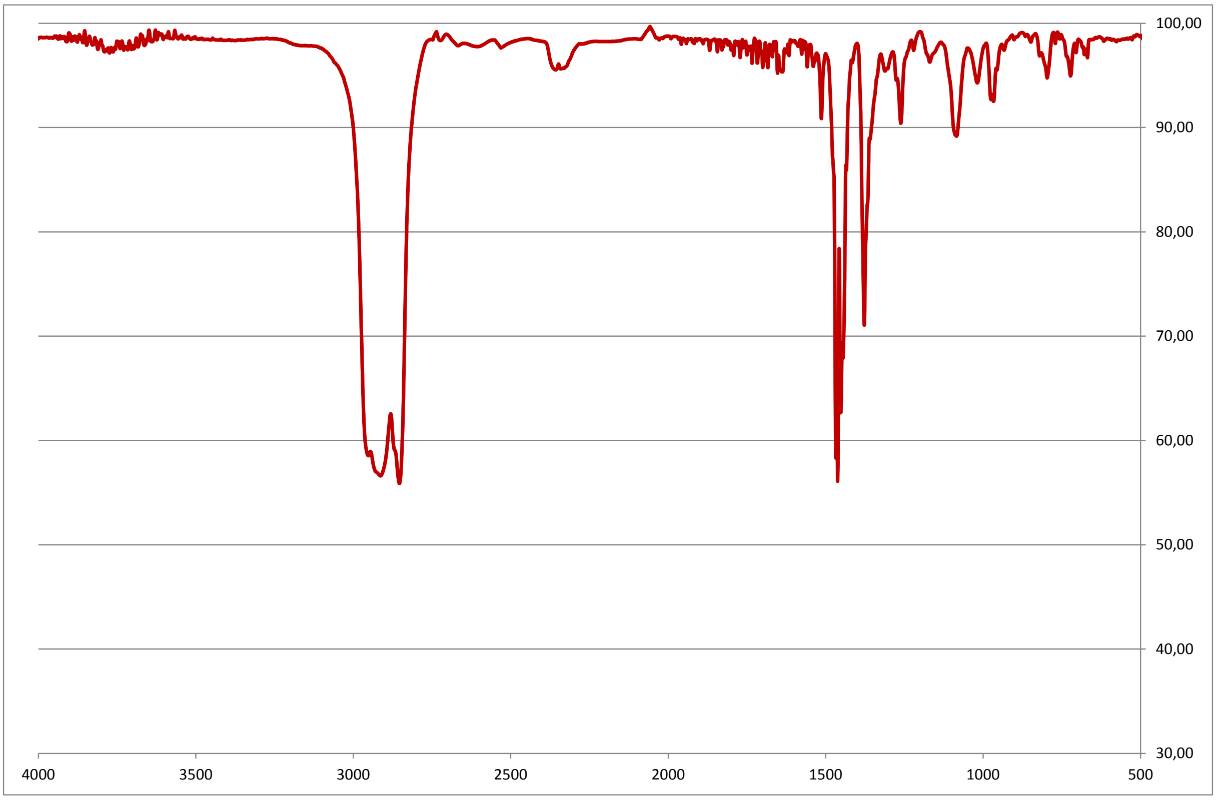

C. ESI-MS spectrometry data

Figure S17. ESI-MS spectrum of microcrystalline dark green material from the photo-driven decomposition of **1**. The material has a very low solubility in THF, and impurities might be more soluble than **3**. Therefore this analysis might not be representative of the whole sample. The ESI-MS spectrum was collected from this very dilute THF extract after filtration. Peak B at m/z = 1203.5587 corresponds to [**3**+H]$^+$ (Calcd for $C_{70}H_{93}N_6Nb_2$: 1203.5589) ; peak C at m/z = 1259.6199 corresponds to [(½ **3**) + **2** + H]$^+$ (Calcd for $C_{74}H_{101}N_6Nb_2$: 1259.6215) ; peak D at m/z = 1315.6820 corresponds to [(2 **2**) + H]$^+$ (Calcd for $C_{78}H_{109}N_6Nb_2$: 1315.6841).

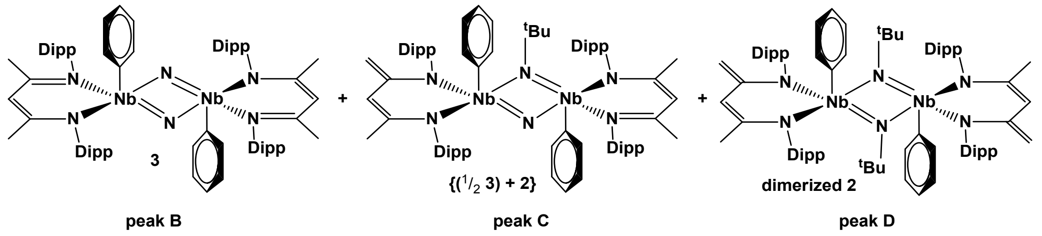

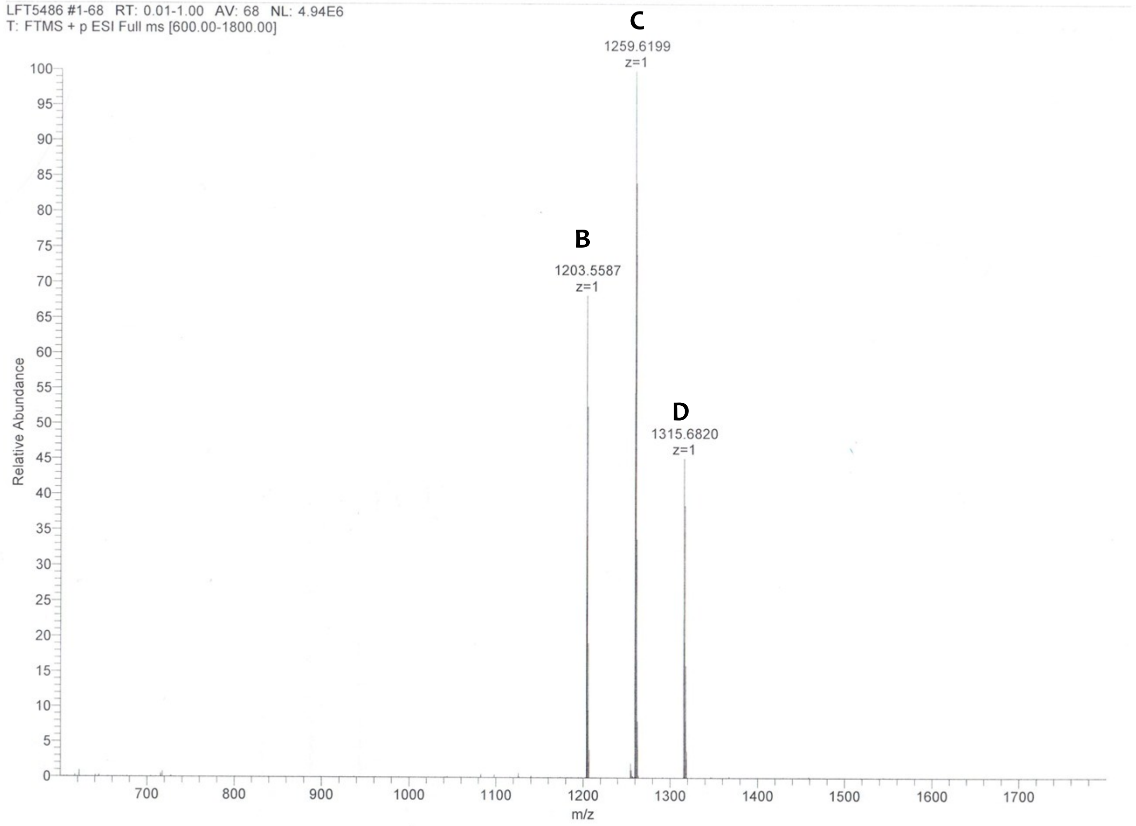

D. X-ray crystallography

X-ray structural determinations were performed on a Bruker SMART QUAZAR diffractometer which is a 3-circle diffractometer that couple a CCD detector with a sealed-tube source of monochromated Mo Ka radiation (λ = 0.71073 Å). A crystal of appropriate size was coated in Paratone-N oil and mounted on a Kapton® loop. The loop was transferred to the diffractometer, centered in the beam, and cooled by a nitrogen flow low-temperature apparatus that had been previously calibrated by a thermocouple placed at the same position as the crystal. Preliminary orientation matrices and cell constants were determined by collection of 60 10 s frames, followed by spot integration and least-squares refinement. The reported cell dimensions were calculated from all reflections with $I > 10\ \sigma$. The data were corrected for Lorentz and polarization effects; no correction for crystal decay was applied. An empirical absorption correction based on comparison of redundant and equivalent reflections was applied using SADABS.[2] All software used for diffraction data processing and crystal-structure solution and refinement are contained in the APEX2 program suite (Bruker AXS, Madison, WI).[3] Thermal parameters for all non-hydrogen atoms were refined anisotropically. For all structures, $R_1 = \Sigma(|F_o| - |F_c|)/\Sigma(|F_o|)$; $wR_2 = [\Sigma\{w(F_o^2 - F_c^2)^2\}/\Sigma\{w(F_o^2)^2\}]^{1/2}$. Thermal ellipsoid plots were created using Mercury supplied with Cambridge Structural Database (CCDC: Cambridge, U.K., 2004-2009).

D.1 Ortep view of compound 2.

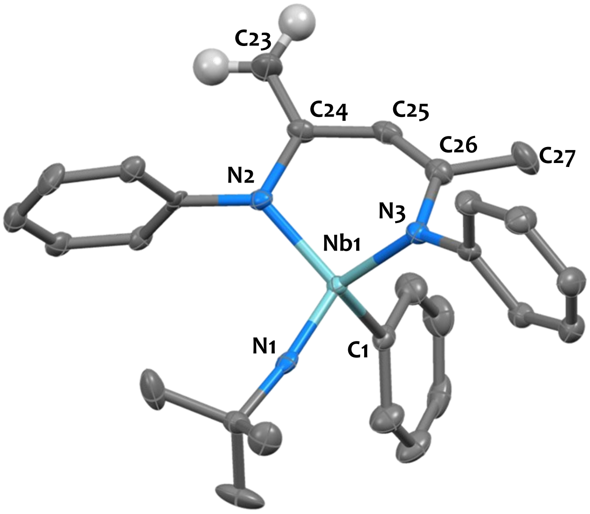

Figure S18. Solid-state molecular structure of [(BDI$^\#$)Nb(N^{t}Bu)(Ph)] **2**. Interstitial solvent molecules, hydrogen atoms (with the exception of the β-methylene group), and diisopropyl aryl groups of the BDI ligands have been omitted for clarity. Niobium (light blue), nitrogen (blue), hydrogen (white) and carbon (grey) atoms are represented with 50% probability ellipsoids. The BDI$^\#$ ligand features a diene-type structure with C23=C24 and C25=C26 double bonds (1.352(7) and 1.373(7) Å resp.) and C24-C25 and C26-C27 single bonds (1.463(8) and 1.499(8) Å resp.). The increased charge density at the BDI$^\#$ ligand is further attested by the short Nb-N$_{BDI\#}$ bond

---

[2] SADABS: Bruker-Nonius Area Detector Scaling and Absorption, **2003**.

[3] Sheldrick, G. M. *Acta Crystallogr. Sect. A* **2008**, *64*, 112–122.

distances (Nb1-N2 = 1.996(4) Å ; Nb1-N3 = 2.005(4) Å) compared to that of related d^0 (BDI)Nb(N^{t}Bu) complexes (2.10-2.42 Å).[4]

D.2 Ortep view of compound 6.

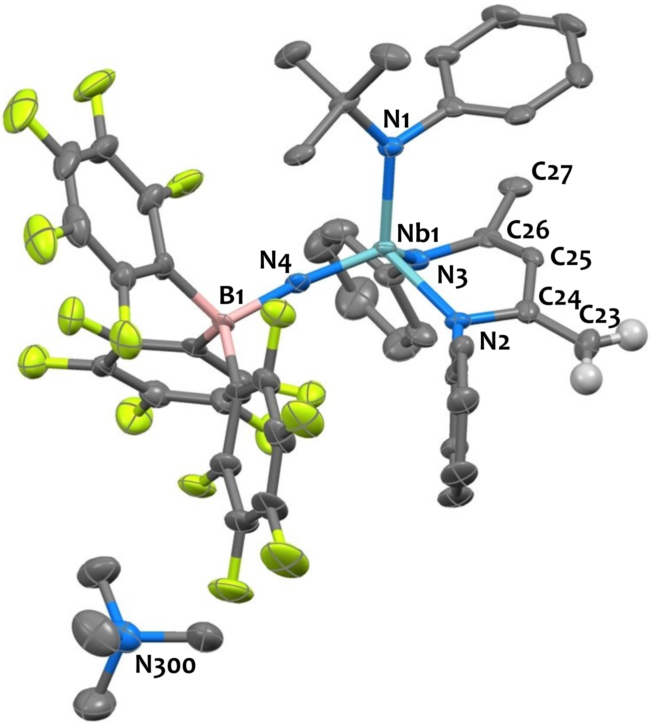

Figure S19. Solid-state molecular structure of **6** $[NMe_4][(BDI^{\#})Nb(N(Ph)^tBu)(NB(C_6F_5)_3)]$. Only one of the two crystallographically nonequivalent but chemically equivalent independent complexes from the asymmetric unit is represented. Interstitial solvent molecules, hydrogen atoms (with the exception of the β-methylene group) and diisopropyl aryl groups of the BDI ligands have been omitted for clarity. Niobium (light blue), boron (pink), fluorine (green), nitrogen (blue), hydrogen (white) and carbon (grey) atoms are represented with 50% probability ellipsoids. Selected bond lengths (Å) and angles (°): B1-N4 1.568(8), N1-Nb1 2.045(5), N2-Nb1 2.068(5), N3-Nb1 2.051(5), N4-Nb1 1.752(5), C23-C24 1.323(9), C24-N2 1.414(8), C24-C25 1.495(9), C25-C26 1.347(9), C26-N3 1.405(8), C26-C27 1.499(9), B1-N4-Nb1 172.8(4).

---

[4] (a) Camp, C.; Maron, L.; Bergman, R. G.; Arnold, J. *J. Am. Chem. Soc.* **2014**, *136*, 17652–17661; (b) Tomson, N. C.; Arnold, J.; Bergman, R. G. *Organometallics* **2010**, *29*, 2926–2942; (c) Obenhuber, A. H.; Gianetti, T. L.; Berrebi, X.; Bergman, R. G.; Arnold, J. *J. Am. Chem. Soc.* **2014**, *136*, 2994–2997.

D.3 Structural parameters

Selected bond lengths (Å) and angles (°) for compounds 1-5:

Compound **1**: C1-Nb1 2.153(3); N1-Nb1 1.767(2); N2-Nb1 2.133(2); N3-Nb1 2.285(2); N4-N5 1.197(3); N4-Nb1 2.050(3); N5-N6 1.147(3); C7-N1-Nb1 161.5(2); N5-N4-Nb1 175.0(2); N6-N5-N4 179.6(4).

Compound **2**: C1-Nb1 2.194(5); N1-Nb1 1.752(4); N2-Nb1 1.996(4); N3-Nb1 2.005(4); C23-C24 1.352(7); C24-C25 1.463(8); C25-C26 1.373(7); C26-C27 1.499(8); C24-N2 1.408(6); C26-N3 1.418(7).

Compound **3**: C1-Nb1 2.165(4); N1-Nb1 1.963(2); N2-Nb1 2.235(2); Nb-N1-Nb1 90.07(13); N1-Nb1-Nb1 44.97(6); N2-Nb1-Nb1 129.66(5).

Compound **4**: C1-Nb1 2.144(2); N1-Nb1 1.7529(16); N2-Nb1 2.0790(16); N3-Nb1 2.2673(15); N4-Nb1 2.2155(17); N4-N5 1.159(2); N5-N6 1.186(2); N6-B1 1.606(3); N5-N4-Nb1 171.24(15); N4-N5-N6 174.70(19); N5-N6-B1 127.77(16).

Compound **5**: N1-Nb1 1.999(2); N2-Nb1 2.097(2); N3-Nb1 2.110(2); N4-Nb1 1.7381(19); B1-N4 1.568(3); B1-N4-Nb1 176.37(17).

Table S.1 Crystallographic parameters for complexes **1**-**4.**

Compound	**1**	**2**	**3.(C_6H_6)**	**4**
Formula	$C_{39}H_{55}N_6Nb$	$C_{39}H_{54}N_3Nb$	$C_{99}H_{150}N_9Nb_3P_{12}$	$C_{57}H_{55}B_1F_{15}N_6Nb$
cryst syst	Monoclinic	Triclinic	Orthorhombic	Triclinic
space group	$P2_1/n$	P-1	Pnnm	P-1
volume (Å^3)	3738.3(3)	905.11(6)	3314.2(2)	2743.4(2)
a (Å)	11.6490(6)	9.6363(4)	12.4801(5)	12.2684(5)
b (Å)	18.9555(10)	10.3540(4)	13.7720(5)	12.7008(5)
c (Å)	17.0768(9)	10.4978(4)	19.2824(8)	19.2268(8)
α (deg)	90	107.0190(10)	90	79.4526(19)
β (deg)	97.526(2)	113.6050(10)	90	83.1067(17)
γ (deg)	90	91.5850(10)	90	68.9230(16)
Z	4	1	2	2
formula weight (g/mol)	700.80	657.76	1281.42	1212.79
density (g cm^{-3})	1.245	1.207	1.284	1.468
absorption coefficient (mm^{-1})	0.356	0.361	0.393	0.315
F(000)	1488	350	1356	1240
temp (K)	100(2)	100(2)	100(2)	100(2)
total no. reflections	41292	12336	56485	61535
unique reflections [R(int)]	6818 [0.061]	5814 [0.036]	3160 [0.127]	10077 [0.033]
Final R indices [I > 2σ(I)]	R1 = 0.0400, wR2 = 0.0824	R1 = 0.0393, wR2 = 0.0786	R1 = 0.0406, wR2 = 0.0988	R1 = 0.0311, wR2 = 0.0749
Largest diff. peak and hole (e.A^{-3})	0.570 and -0.562	0.455 and -0.304	0.831 and -1.023	0.441 and -0.339
GoF	1.071	1.057	1.097	1.060

Table S.2 Crystallographic parameters for complexes **5** to **6.**

Compound	**5.$(CH_3C_6H_5)_{0.5}$**	**6.(C_6H_6)**
Formula	$C_{60.5}H_{59}B_1F_{15}N_4Nb$	$C_{67}H_{72}B_1F_{15}N_5Nb$
cryst syst	Orthorhombic	Triclinic
space group	Pbca	P-1
volume (Å^3)	11075.2(6)	6241.6(7)
a (Å)	19.3473(5)	12.5396(9)
b (Å)	22.4336(7)	17.4757(11)
c (Å)	25.5172(9)	29.990(2)
α (deg)	90	84.127(3)
β (deg)	90	82.987(3)
γ (deg)	90	73.602(3)
Z	8	4
formula weight (g/mol)	1230.84	1336.01
density (g cm^{-3})	1.476	1.422
absorption coefficient (mm^{-1})	0.312	0.283
F(000)	5048	2760
temp (K)	100(2)	100(2)
total no. reflections	159023	58734
unique reflections [R(int)]	10157 [0.072]	22438 [0.081]
Final R indices [I > 2σ(I)]	R1 = 0.0360, wR2 = 0.9055	R1 = 0.0799, wR2 = 0.2127
Largest diff. peak and hole (e.A^{-3})	0.843 and -0.323	1.753 and -0.808
GoF	1.059	1.025

E. UV-visible spectra

Figure S20. Solution UV/visible absorption spectra (298 K) of complexes **1** (green line) and **4** (red line) recorded from Et_2O solutions.

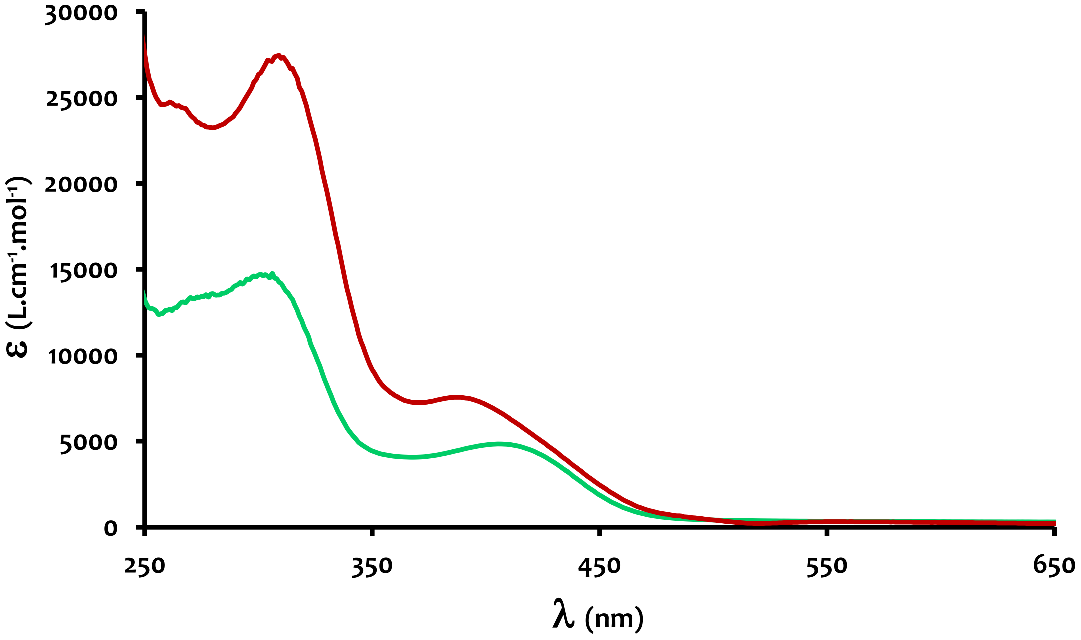

The interesting photoreactivity observed for **1** and **4** made it of interest to measure their UV-Vis spectra. The collected data for these d^0 species are presented in Figure S20. Both compounds display high-intensity (ε = 27500 and 14700 $L.cm^{-1}.mol^{-1}$ for **1** and **4** respectively) electronic transitions in the UV region around 305 nm. Additionally, lower intensity absorption bands are observed near the visible region at λ = 387 nm for **1** (ε = 7560 $L.cm^{-1}.mol^{-1}$) and λ = 404 nm for **4** (ε = 4840 $L.cm^{-1}.mol^{-1}$), responsible for yellow-orange colors of these molecules. Since **1** and **4** are both d^0 species and given the measured intensities we attribute these transition to intraligand π→π* and/or LMCT transitions. We reported related transitions in d^0 Nb (BDI) imido species: see C. Camp et al., *J. Am. Chem. Soc.* **2014**, 136(*50*), 17652-17661.